CHAPTER 6

THERMOELASTIC DAMPING ANALYSIS FOR SIZE-DEPENDENT MICROPLATE RESONATORS UTILIZING MODIFIED COUPLE STRESS THEORY AND THREE-PHASE-LAG HEAT CONDUCTION MODEL

6.1 Introduction[1]

The dynamic properties and behavior of microplate resonators have been experimentally shown to be size-dependent. The thermoelastic damping (TED) plays an important role on the inherent energy dissipation of the microplate resonators. The present chapter is concerned with the study of size-dependent TED in microplate resonators on the basis of modified couple stress theory (MCST) and three-phase-lag (TPL) thermoelastic model. Kirchhoff's plate theory is employed for the formulation of the plate problem.

In the past, several investigations on TED addressing microplate resonators have been done. Zhong et al. (2014) established the formula of the quality factor for TED in microplate resonators by deriving the governing equation of motion with the help of Hamilton's principle. Zuo et al. (2016) carried out analytical modeling of TED in bilayered microplate resonators. analyzed small scale effect on TED in microplate resonators

[1]The content of this chapter is published in ***International Journal of Heat and Mass Transfer***, 148 (2020):118997.

in the framework of MCST and the generalized dual-phase-lag (DPL) heat conduction model. Aghazadeh et al. (2018) studied about the thermal effect on bending, buckling and free vibration of functionally graded rectangular microplates possessing a variable length scale parameter. Najafi et al. (2018) illustrated TED in a fully clamped rectangular microplate and solved the coupled thermoelastic equations with the help of Galerkin method. Zhou and Li (2021) investigated TED in rectangular and circular micro and nanoplate resonators considering nonlocal DPL heat conduction model. Borjalilou and Asghari (2018; 2021) have also considered the DPL heat conduction model to study the size effects on TED in microplate resonators. Yang et al. (2021) presented a generalized methodology for TED in axisymmetric vibration of circular plate resonators covered by multiple partial coatings. Based on modified nonlocal strain gradient theory and nonlocal heat conduction law, Ge at al. (2021) analyzed TED in rectangular micro and nanoplate resonators. A detailed review on the size-dependent models of microbeam and microplate reported by Kong (2021) can also be referred in this respect.

Being motivated from above works, this chapter presents a detail analysis of the quality factor for TED in microplate resonators under TPL heat conduction model. The variations of TED as functions of the normalized frequency, microplate thickness, and length-scale parameter have been investigated. The effect of phase-lag parameters on TED has also been discussed. The results of the present model are compared to the existing results of the classical continuum theory. The present work investigates that MCST with small values of phase-lag parameters can increase the quality factor of microplate resonators with a smaller thickness.

6.2 Formulation

A rectangular microplate resonator of length L $(0 \leq x \leq L)$, width b $(0 \leq y \leq b)$, and thickness h $\left(-\frac{h}{2} \leq z \leq +\frac{h}{2}\right)$ is considered to investigate TED as shown in Figure 6.2.1.

Denoting $w(x, y, t)$ as the transverse deflection of the microplate at time t, the components of displacement field based on Kirchhoff plate theory (Timoshenko and Woinowsky-Krieger, 1959; Reddy, 1999) can be expressed as:

$$u_x = -z\frac{\partial w(x, y, t)}{\partial x},\ u_y = -z\frac{\partial w(x, y, t)}{\partial y},\ u_z = w(x, y, t) \tag{6.2.1}$$

in which u_x, u_y, and u_z represent the displacements at any point (x, y, z) in x, y, and $z-$directions, respectively.

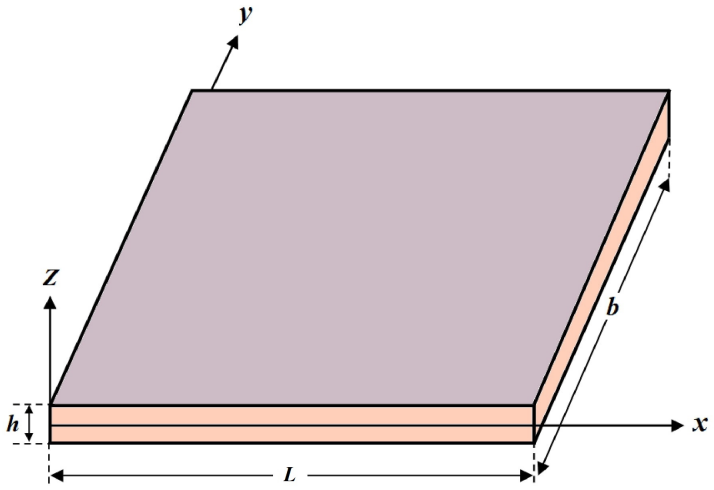

Figure 6.2.1: Schematic diagram of a rectangular microplate.

6.2.1 The TPL heat conduction model

The generalized constitutive relation of three-phase-lagging heat conduction model that captures the microscopic effects in heat transport phenomenon as introduced by Roychoudhuri (2007) is given by

$$q(\boldsymbol{r}, t + \tau_q) = -\left[k\nabla T(\boldsymbol{r}, t + \tau_T) + k^*\nabla \upsilon(\boldsymbol{r}, t + \tau_\upsilon)\right] \tag{6.2.2}$$

Here, ∇T is the temperature gradient at a point $\mathring{\boldsymbol{P}}$ of the material at time $t+\tau_T$ corresponding to the heat flux vector q at the same point at the time $t+\tau_q$. The thermal displacement gradient $\nabla \upsilon$ established across a material at point $\mathring{\boldsymbol{P}}$ at time $t+\tau_\upsilon$ results in heat flux to flow at a different instant of time τ_q.

Taking Taylor series expansion on both sides of Eq. (6.2.2) and retaining the terms up to the second order in τ_q and the first order in τ_T and τ_υ, the constitutive relation under TPL heat conduction takes the form

$$\dot{q}+\tau_q\ddot{q}+\frac{\tau_q^2}{2}\dddot{q}=-\left[(k+k^*\tau_\upsilon)\nabla\dot{T}+k\tau_T\nabla\ddot{T}+k^*\nabla T\right] \tag{6.2.3}$$

From Eqs. (2.2.3) and (6.2.3), one can obtain the heat conduction equation with three-phase-lagging effect as

$$k^*\nabla^2 T+(k+k^*\tau_\upsilon)\nabla\dot{T}+k\tau_T\nabla^2\ddot{T}=\left(1+\tau_q\frac{\partial}{\partial t}+\frac{\tau_q^2}{2}\frac{\partial^2}{\partial t^2}\right)\left(\rho C_v\ddot{T}+\frac{TE\alpha_T}{(1-2\nu)}\frac{\partial^2\epsilon}{\partial t^2}\right) \tag{6.2.4}$$

Above equation further can be rewritten as:

$$\left(k^*+(k+k^*\tau_\upsilon)\frac{\partial}{\partial t}+k\tau_T\frac{\partial^2}{\partial t^2}\right)\nabla^2\theta=\left(1+\tau_q\frac{\partial}{\partial t}+\frac{\tau_q^2}{2}\frac{\partial^2}{\partial t^2}\right)\left(\rho C_v\ddot{\theta}+\frac{T_0E\alpha_T}{(1-2\nu)}\frac{\partial^2\epsilon}{\partial t^2}\right) \tag{6.2.5}$$

It is notable that the thermal gradients along the $z-$direction are much larger than the gradients along the x and $y-$directions in thin plates (Lifshitz and Roukes, 2000). Therefore, in above equation the term $\nabla^2\theta$ can be replaced by $\partial^2\theta/\partial z^2$. Hence, Eq. (6.2.5) reduces to

$$\left(k^*+(k+k^*\tau_\upsilon)\frac{\partial}{\partial t}+k\tau_T\frac{\partial^2}{\partial t^2}\right)\frac{\partial^2\theta}{\partial z^2}=\left(1+\tau_q\frac{\partial}{\partial t}+\frac{\tau_q^2}{2}\frac{\partial^2}{\partial t^2}\right)\left(\rho C_v\frac{\partial^2\theta}{\partial t^2}+\frac{T_0E\alpha_T}{(1-2\nu)}\frac{\partial^2\varepsilon}{\partial t^2}\right) \tag{6.2.6}$$

Based on the MCST, the non-zero components of the strain and symmetric part of

the rotation gradient tensors can be expressed as:

$$\epsilon_{xx} = -z\frac{\partial^2 w}{\partial x^2},\ \epsilon_{yy} = -z\frac{\partial^2 w}{\partial y^2},\ \epsilon_{xy} = -z\frac{\partial^2 w}{\partial x \partial y} \tag{6.2.7}$$

$$\chi_{xx} = \frac{\partial^2 w}{\partial x \partial y},\ \chi_{yy} = \frac{\partial^2 w}{\partial x \partial y},\ \chi_{xy} = \frac{1}{2}\left(\frac{\partial^2 w}{\partial y^2} - \frac{\partial^2 w}{\partial x^2}\right),\ \chi_{xz} = \chi_{yz} = \chi_{zz} = 0, \tag{6.2.8}$$

It is worth to note that we have considered plane stress condition and hence $\sigma_{zz} = 0$. From Eq. (3.2.6), one can obtain

$$\left.\begin{aligned} \sigma_{xx} &= \tfrac{E}{1-\nu^2}\left(\epsilon_{xx} + \nu\epsilon_{yy}\right) - \tfrac{1}{1-\nu}\alpha_T\theta \\ \sigma_{yy} &= \tfrac{E}{1-\nu^2}\left(\epsilon_{yy} + \nu\epsilon_{xx}\right) - \tfrac{1}{1-\nu}\alpha_T\theta \\ \epsilon_{zz} &= -\tfrac{\nu}{1-\nu}\left(\epsilon_{xx} + \epsilon_{yy}\right) + \tfrac{1+\nu}{1-\nu}\alpha_T\theta \end{aligned}\right\} \tag{6.2.9}$$

Now, using Eq. (6.2.7) into Eq. (6.2.9), we obtain

$$\left.\begin{aligned} \sigma_{xx} &= -\tfrac{Ez}{1-\nu^2}\left(\tfrac{\partial^2 w}{\partial x^2} + \nu\tfrac{\partial^2 w}{\partial y^2}\right) - \tfrac{1}{1-\nu}E\alpha\theta \\ \sigma_{yy} &= -\tfrac{Ez}{1-\nu^2}\left(\tfrac{\partial^2 w}{\partial y^2} + \nu\tfrac{\partial^2 w}{\partial x^2}\right) - \tfrac{1}{1-\nu}E\alpha_T\theta \\ \epsilon_{zz} &= \tfrac{\nu z}{1-\nu}\left(\tfrac{\partial^2 w}{\partial x^2} + \tfrac{\partial^2 w}{\partial y^2}\right) + \tfrac{1+\nu}{1-\nu}\alpha_T\theta \end{aligned}\right\} \tag{6.2.10}$$

By inserting Eqs. (6.2.7) and (6.2.8) into Eq. (3.2.1), the variation of strain energy (U) of microplate resonator can be written as:

$$\begin{aligned} \delta U = \int_0^b \int_0^a \Bigg[&-M_{xx}\delta\left(\frac{\partial^2 w}{\partial x^2}\right) - M_{yy}\delta\left(\frac{\partial^2 w}{\partial y^2}\right) - 2M_{xy}\delta\left(\frac{\partial^2 w}{\partial x \partial y}\right) \\ &+ Y_{xx}\delta\left(\frac{\partial^2 w}{\partial x \partial y}\right) - Y_{yy}\delta\left(\frac{\partial^2 w}{\partial x \partial y}\right) + Y_{xy}\delta\left(\frac{\partial^2 w}{\partial y^2}\right) - Y_{xy}\delta\left(\frac{\partial^2 w}{\partial x^2}\right)\Bigg] dxdy \end{aligned} \tag{6.2.11}$$

where M_{xx}, M_{xy}, and M_{yy} are the resultants of stress and Y_{xx}, Y_{xy}, and Y_{yy} are the

resultants of couple stress defined as follows:

$$M_{xx} = \int_{-\frac{h}{2}}^{+\frac{h}{2}} z\sigma_{xx}dz,\ M_{yy} = \int_{-\frac{h}{2}}^{+\frac{h}{2}} z\sigma_{yy}dz,\ M_{xy} = \int_{-\frac{h}{2}}^{+\frac{h}{2}} z\sigma_{xy}dz \tag{6.2.12}$$

$$Y_{xx} = \int_{-\frac{h}{2}}^{+\frac{h}{2}} m_{xx}dz,\ Y_{yy} = \int_{-\frac{h}{2}}^{+\frac{h}{2}} m_{yy}dz,\ Y_{xy} = \int_{-\frac{h}{2}}^{+\frac{h}{2}} m_{xy}dz \tag{6.2.13}$$

where

$$m_{xx} = 2\mu l^2 \frac{\partial^2 w}{\partial x \partial y},\ m_{yy} = -2\mu l^2 \frac{\partial^2 w}{\partial x \partial y},\ m_{xy} = \mu l^2 \left(\frac{\partial^2 w}{\partial y^2} - \frac{\partial^2 w}{\partial x^2}\right) \tag{6.2.14}$$

Combining Eqs.(6.2.7), (6.2.8), (6.2.10), (6.2.12), and (6.2.13), we find the expressions for the stress resultants in terms of the deflection of the plate in the thermoelastic conditions as follows:

$$\begin{Bmatrix} M_{xx} \\ M_{yy} \\ M_{xy} \end{Bmatrix} = -D \begin{bmatrix} 1 & \nu & 0 \\ \nu & 1 & 0 \\ 0 & 0 & 1-\nu \end{bmatrix} \begin{Bmatrix} w_{xx} \\ w_{yy} \\ w_{xy} \end{Bmatrix} - \frac{1}{1-\nu} \begin{Bmatrix} M_T \\ M_T \\ 0 \end{Bmatrix} \tag{6.2.15}$$

$$\begin{Bmatrix} Y_{xx} \\ Y_{yy} \\ Y_{xy} \end{Bmatrix} = \mu l^2 h \begin{bmatrix} 0 & 0 & 2 \\ 0 & 0 & -2 \\ -1 & 1 & 0 \end{bmatrix} \begin{Bmatrix} w_{xx} \\ w_{yy} \\ w_{xy} \end{Bmatrix} \tag{6.2.16}$$

where $D = Eh^3/12\,(1-\nu^2)$ is known as the bending rigidity of the plate. In above Eq. (6.2.15), the parameter M_T is called the thermal moment given by

$$M_T = E\alpha_T \int_{-\frac{h}{2}}^{+\frac{h}{2}} \theta z dz \tag{6.2.17}$$

The variation of the kinetic energy (K) can be written as:

$$\delta K = \rho h \int_0^b \int_0^a \frac{\partial w}{\partial t} \delta \left(\frac{\partial w}{\partial t}\right) dxdy \tag{6.2.18}$$

On the basis of the Hamilton's principle (Dym and Shames, 1984), the equation of motion of the microplate resonators on the time interval $[t_1, t_2]$ is given by

$$\int_{t_1}^{t_2} (\delta U - \delta K)\, dt = 0 \tag{6.2.19}$$

By substituting Eqs. (6.2.11) and (6.2.18) into Eq. (6.2.19) and using Green's theorem, the equation of motion of the microplate takes the form

$$\frac{\partial^2 M_{xx}}{\partial x^2} + 2\frac{\partial^2 M_{xy}}{\partial x \partial y} + \frac{\partial^2 M_{yy}}{\partial y^2} - \frac{\partial^2 Y_{xx}}{\partial x \partial y} + \frac{\partial^2 Y_{xy}}{\partial x^2} - \frac{\partial^2 Y_{xy}}{\partial y^2} + \frac{\partial^2 Y_{yy}}{\partial x \partial y} - \rho h \frac{\partial^2 w}{\partial t^2} = 0 \tag{6.2.20}$$

where ρ denotes the density of the material of the microplate. Now, using Eqs. (6.2.15) and (6.2.16) into Eq. (6.2.20), the governing equation of motion of the microplate can be expressed in terms of the deflection function w as:

$$\left(D + \mu l^2 h\right)\left(\frac{\partial^4 w}{\partial x^4} + 2\frac{\partial^4 w}{\partial x^2 \partial y^2} + \frac{\partial^4 w}{\partial y^4}\right) + \frac{1}{1-\nu}\left(\frac{\partial^2 M_T}{\partial x^2} + \frac{\partial^2 M_T}{\partial y^2}\right) + \rho h \frac{\partial^2 w}{\partial t^2} = 0 \tag{6.2.21}$$

Above equation consists of three parts: the first part associated with D and ρh are as in classical plate model; the second part containing $\mu l^2 h$ represents the size-effect and the third part consisting M_T is due to the effect of thermoelasticity coupling. In the second part, the parameter l enables to content the material size features in the new model and due to this parameter it is possible to explain the size-effects on TED in the present context. Furthermore, if we take $l = 0$, the new model reduces to the classical thermoelastic plate model (Rezazadeh, 2009) in which the size-effect is not considered. Substituting Eq. (6.2.7) into the coupled heat conduction equation (5.2.2), is obtained

as:

$$\chi\left[\frac{k^*}{k}\left(1+\tau_\upsilon\frac{\partial}{\partial t}\right)+\left(\frac{\partial}{\partial t}+\tau_T\right)\right]\frac{\partial^2\theta}{\partial z^2}=\left(1+2\Delta_E\frac{(1+\nu)}{(1-2\nu)(1-\nu)}\right)\left(1+\tau_q\frac{\partial}{\partial t}+\frac{\tau_q^2}{2}\frac{\partial^2}{\partial t^2}\right)\frac{\partial^2\theta}{\partial t^2}$$
$$-\frac{\Delta_E z}{\alpha_T(1-\nu)}\left(1+\tau_q\frac{\partial}{\partial t}+\frac{\tau_q^2}{2}\frac{\partial^2}{\partial t^2}\right)\left(\frac{\partial^4 w}{\partial t^2\partial x^2}+\frac{\partial^4 w}{\partial t^2\partial y^2}\right) \tag{6.2.22}$$

Further, above equation can be simplified to

$$\chi\left[\frac{k^*}{k}\left(1+\tau_\upsilon\frac{\partial}{\partial t}\right)+\left(\frac{\partial}{\partial t}+\tau_T\right)\right]\frac{\partial^2\theta}{\partial z^2}=\left(1+\tau_q\frac{\partial}{\partial t}+\frac{\tau_q^2}{2}\frac{\partial^2}{\partial t^2}\right)\frac{\partial^2\theta}{\partial t^2}$$
$$-\frac{\Delta_E z}{\alpha_T(1-\nu)}\left(1+\tau_q\frac{\partial}{\partial t}+\frac{\tau_q^2}{2}\frac{\partial^2}{\partial t^2}\right)\left(\frac{\partial^4 w}{\partial t^2\partial x^2}+\frac{\partial^4 w}{\partial t^2\partial y^2}\right) \tag{6.2.23}$$

Hence, Eqs. (6.2.21) and (6.2.23) constitute the basic governing equations of the present problem of microplate resonator that incorporate the size-effect and the three-phase-lagging effect.

6.3 Solution of the problem

To find the influence of thermoelastic coupling on harmonic vibrations of the microplate resonator, we solve coupled thermoelastic Eqs. (6.2.21) and (6.2.23) for the case of simple- harmonic vibrations. Firstly, we assume that the solution for w and θ can be expressed as:

$$w(x,\,y,\,t)=\widehat{W}(x,\,y)\,e^{i\omega t},\quad \theta(x,\,y,\,z,\,t)=\widehat{\theta}(x,\,y,\,z)\,e^{i\omega t} \tag{6.3.1}$$

where ω is angular frequency of vibrations, $\widehat{W}$ and $\widehat{\theta}$ are complex-valued functions. Hence, substituting Eq. (6.3.1) into Eq. (6.2.23), we arrive at the following equation

$$\frac{\partial^2\widehat{\theta}}{\partial z^2}+p_4^2\widehat{\theta}=p_4^2\frac{\Delta_E}{\alpha_T\left(1-\nu\right)}z\left(\frac{\partial^2\widehat{W}}{\partial x^2}+\frac{\partial^2\widehat{W}}{\partial y^2}\right) \tag{6.3.2}$$

where

$$p_4^2=\frac{\omega}{\chi}\frac{\left(\omega+i\tau_q\omega^2-\frac{\tau_q^2}{2}\omega^3\right)}{\left[\frac{k^*}{k}+i\left(\frac{k^*\tau_v}{k}+1\right)\omega-\omega^2\tau_T\right]} \tag{6.3.3}$$

The complex parameter p_4 can be simplified in the following form:

$$p_4=\sqrt{\frac{\omega}{\chi}}\sqrt{d_1+id_2}=\frac{\xi}{h}\left(\eta_4+i\frac{\eta_5}{|d_2|}d_2\right) \tag{6.3.4}$$

where

$$\xi=h\sqrt{\frac{\omega}{2\chi}},\ \eta_4=\sqrt{\sqrt{d_1^2+d_2^2}+d_1},\ \eta_5=\sqrt{\sqrt{d_1^2+d_2^2}-d_1} \tag{6.3.5}$$

$$d_1=\frac{\omega\left[\frac{k^*}{k}+\left\{\left(\tau_q-\tau_T\right)+\frac{k^*\tau_q\tau_v}{k}-\frac{k^*\tau_q^2}{2k}\right\}\omega^2+\frac{\tau_q^2\tau_T}{2}\omega^4\right]}{\left[\left(\omega+\frac{k^*\tau_v\omega}{k}\right)^2+\left(\frac{k^*}{k}-\tau_T\omega^2\right)^2\right]}$$

$$d_2=\frac{\omega\left[\left\{\frac{k^*\tau_q}{k}+\frac{k^*\tau_v}{k}-1\right\}\omega+\left\{\frac{k^*\tau_q^2\tau_v}{2k}+\frac{\tau_q^2}{2}-\tau_q\tau_T\right\}\omega^3\right]}{\left[\left(\omega+\frac{k^*\tau_v\omega}{k}\right)^2+\left(\frac{k^*}{k}-\tau_T\omega^2\right)^2\right]}$$

The general solution of Eq. (6.3.2) for temperature function $\widehat{\theta}$ is given by

$$\widehat{\theta}\left(x,\,y,\,z\right)=E_1\,sin\left(p_4z\right)+E_2\,cos\left(p_4z\right)+\frac{\Delta_E}{\alpha_T\left(1-\nu\right)}z\left(\frac{\partial^2\widehat{W}}{\partial x^2}+\frac{\partial^2\widehat{W}}{\partial y^2}\right) \tag{6.3.6}$$

where E_1 and E_2 are arbitrary constants to be determined by applying thermal boundary conditions at the upper and lower surfaces of the plate. Suppose, these two surfaces are adiabatic and in this case, one can obtain the temperature in the plate as:

$$\widehat{\theta}\left(x,\,y,\,z\right)=\frac{\Delta_E}{\alpha_T\left(1-\nu\right)}z\left(\frac{\partial^2\widehat{W}}{\partial x^2}+\frac{\partial^2\widehat{W}}{\partial y^2}\right)\left[z-\frac{sin\left(p_4z\right)}{p\,cos\left(\frac{p_4h}{2}\right)}\right] \tag{6.3.7}$$

By using Eqs. (6.2.17), (6.2.21), (6.3.1), and (6.3.7), the equation of motion can be written as

$$\rho h\omega^2\widehat{W} = \left\{D + \mu l^2 h + \frac{Eh^3}{12\left(1-\nu\right)^2}\Delta_E\left[1 + f\left(\omega\right)\right]\right\}\left(\frac{\partial^4\widehat{W}}{\partial x^4} + 2\frac{\partial^4\widehat{W}}{\partial x^2\partial y^2} + \frac{\partial^4\widehat{W}}{\partial y^4}\right) \tag{6.3.8}$$

where

$$f\left(\omega\right) = \frac{24}{\left(hp_4\right)^3}\left[\frac{hp_4}{2} - tan\left(\frac{hp_4}{2}\right)\right] \tag{6.3.9}$$

Now, we aim to find the eigen frequency, ω_0 with the help of boundary conditions. Noting that the value of ω_0 is highly dependent on the supporting boundary conditions of the plate. Here, firstly we consider boundary conditions of the plate such that the four edges are simply supported. In this case, the deflection function can be written as:

$$\widehat{W}\left(x,\, y\right) = \sum_{m=1}^{\infty}\sum_{n=1}^{\infty} B_{mn}\, sin\left(\frac{m\pi}{L}x\right)\, sin\left(\frac{n\pi}{b}y\right) \tag{6.3.10}$$

where B_{mn} is a constant and m and n are mode numbers. Substituting Eq. (6.3.10) into Eq. (6.3.8), one can obtain

$$\left[\pi^4\left(\frac{m^2}{L^2} + \frac{n^2}{b^2}\right)^2 - \frac{\rho h\omega^2}{D'}\right] B_{mn} sin\left(\frac{m\pi x}{L}\right) sin\left(\frac{n\pi x}{b}\right) = 0 \tag{6.3.11}$$

where $D' = D + \mu l^2 h + \frac{Eh^3}{12(1-\nu)^2}\Delta_E\left[1 + f\left(\omega\right)\right]$. To make the condition (6.3.11) meet each point of the microplate, there must be

$$\pi^4\left(\frac{m^2}{L^2} + \frac{n^2}{b^2}\right)^2 - \frac{\rho h\omega^2}{D'} = 0 \tag{6.3.12}$$

The dispersion relation for the thermoelastic microplate can therefore be obtained as:

$$\omega = \pi^2\sqrt{\frac{D'}{\rho h}}\left(\frac{m^2}{L^2}+\frac{n^2}{b^2}\right) = \pi^2\sqrt{\frac{D+\mu l^2 h}{\rho h}}\left(\frac{m^2}{L^2}+\frac{n^2}{b^2}\right)\sqrt{1+\frac{\frac{Eh^3}{12(1-\nu)^2}\Delta_E\left[1+f\left(\omega\right)\right]}{D+\mu l^2 h}}$$
$$= \omega_0\sqrt{1+\frac{\frac{(1+\nu)}{(1-\nu)}\Delta_E\left[1+f\left(\omega\right)\right]}{1+6\left(1-\nu\right)\left(\frac{l}{h}\right)^2}} = \omega_0\sqrt{1+\frac{\frac{(1+\nu)}{(1-\nu)}\Delta_E\left[1+f\left(\omega\right)\right]}{R}} \tag{6.3.13}$$

where $R = 1+6\left(1-\nu\right)\left(\frac{l}{h}\right)^2$ and ω_0 is isothermal value of eigen frequency of the microplate given by

$$\omega_0 = \pi^2\sqrt{\frac{D+\mu l^2 h}{\rho h}}\left(\frac{m^2}{L^2}+\frac{n^2}{b^2}\right) \tag{6.3.14}$$

Further, we consider the case in which the four opposite edges of microplate are clamped. In this case, the isothermal value of the eigen frequency can be derived as:

$$\omega_0 = \pi^2\sqrt{\frac{D+\mu l^2 h}{\rho h}}\left[\frac{\left(m+\frac{1}{2}\right)^2}{L^2}+\frac{\left(n+\frac{1}{2}\right)^2}{b^2}\right] \tag{6.3.15}$$

Since $\Delta_E \ll 1$, Eq. (6.3.13) can be expanded by Taylor series up to its first order term as follows:

$$\omega = \omega_0\left\{1+\frac{\Delta_E}{2}\frac{\frac{(1+\nu)}{(1-\nu)}}{R}\left[1+f\left(\omega\right)\right]\right\} \tag{6.3.16}$$

Further, considering that the TED is very weak, $f\left(\omega\right)$ can be approximated by $f\left(\omega_o\right)$ in above equation to get the explicit form of above equation as:

$$\omega = \omega_0\left\{1+\frac{\Delta_E}{2}\frac{\frac{(1+\nu)}{(1-\nu)}}{R}\left[1+f\left(\omega_0\right)\right]\right\} \tag{6.3.17}$$

From Eq. (6.3.17), it is found that the frequency ω is complex such that the real part $\left(Re\left(\omega\right)\right)$ gives the new eigen frequencies of the microplate resonators in the presence of thermoelastic coupling, and the imaginary part $\left(Im\left(\omega\right)\right)$ gives the attenuation of the vibration. From Eqs. (6.3.4), (6.3.9), and (6.3.17), the real and imaginary parts of ω

can be separated as:

$$Re\left(\omega\right)=\omega_0\left[1+\frac{\Delta_E}{R}\frac{\left(1+\nu\right)}{2\left(1-\nu\right)}\left\{1+12\frac{\left(\eta_4^2-\eta_5^2\right)}{\xi^2\left(\eta_4^2+\eta_5^2\right)^2}\right.\\ \left.-24\frac{\eta_4\left(\eta_4^2-3\eta_5^2\right)sin\left(\xi\eta_4\right)+\frac{\eta_5}{|d_2|}d_2\left(\eta_5^2-3\eta_4^2\right)sinh\left(\frac{\eta_5\xi d_2}{|d_2|}\right)}{\xi^3\left(\eta_4^2+\eta_5^2\right)^3\left(cos\left(\xi\eta_4\right)+cosh\left(\xi\eta_5\right)\right)}\right\}\right] \tag{6.3.18}$$

$$Im\left(\omega\right)=-\frac{\Delta_E}{R}\frac{12\left(1+\nu\right)}{\left(1-\nu\right)}\omega_0\left[\frac{\eta_5 d_2\eta_4}{|d_2|\,\xi^2\left(\eta_1^2+\eta_2^2\right)^2}\right.\\ \left.-\left\{\frac{\frac{\eta_5}{|d_2|}d_2\left(3\eta_4^2-\eta_5^2\right)sin\left(\xi\eta_4\right)-\eta_4\left(3\eta_5^2-\eta_4^2\right)sinh\left(\frac{\eta_5\xi d_2}{|d_2|}\right)}{\xi^3\left(\eta_4^2+\eta_5^2\right)^3\left(cos\left(\xi\eta_4\right)+cosh\left(\xi\eta_5\right)\right)}\right\}\right] \tag{6.3.19}$$

By inserting Eqs. (6.3.18) and (6.3.19) into Eq. (2.1.12), the amount of TED of microplate resonators on the basis of the MCST with three-phase-lagging effects is finally derived as:

$$Q^{-1}=\left|\frac{24\left(1+\nu\right)}{\left(1-\nu\right)}\frac{\Delta_E}{R}\left[\frac{\eta_5 d_2\eta_4}{|d_2|\,\xi^2\left(\eta_4^2+\eta_5^2\right)^2}\right.\right.\\ \left.\left.-\left\{\frac{\frac{\eta_5}{|d_2|}d_2\left(3\eta_4^2-\eta_5^2\right)sin\left(\xi\eta_4\right)-\eta_4\left(3\eta_5^2-\eta_4^2\right)sinh\left(\frac{\eta_5\xi d_2}{|d_2|}\right)}{\xi^3\left(\eta_4^2+\eta_5^2\right)^3\left(cos\left(\xi\eta_4\right)+cosh\left(\xi\eta_5\right)\right)}\right\}\right]\right| \tag{6.3.20}$$

6.4 Results and discussion

In the previous section, we derived an analytical expression for the TED in microplate resonator on the basis of the MCST in the context of heat conduction with three-phase-lagging effects. In this section, we aim to illustrate the analytical results and investigate the damping effect in the plate resonators. Hence, we present the numerical results by carrying out computer programming and show the variation of TED scaled by Δ_E (i.e.

Q^{-1}/Δ_E) of the Kirchhoff microplate resonator in the context of MCST and TPL heat conduction model. We analyze the influences of some parameters on TED such as normalized frequency, microplate thickness, aspect ratio, length-scale parameter, and boundary conditions. In our study, two different boundary conditions are considered: such as simply supported (SSSS) edges and clamped-clamped (CCCC) edges of the microplate resonators. We also compare the nature of TED predicted by the present couple stress theory with the corresponding results predicted by the classical continuum theory ($l = 0$) . The material of the microplate is considered to be Silicon. The thermal and mechanical properties of Silicon material at reference temperature $300\,K$ are listed below (Li et al., 2012)

$E = 157\,GPa$, $\nu = 0.25$, $k = 148\,Wm^{-1}K^{-1}$, $k^* = 70\,Wm^{-1}K^{-1}s^{-1}$,$\rho = 2330\,Kgm^{-3}$, $C_v = 1.63 \times 10^6 Jm^{-3}K^{-1}$, $\alpha_T = 2.6 \times 10^{-6}K^{-1}$.

The values of phase-lags time are taken as $\tau_q = 3.96 \times 10^{-12}s$, $\tau_T = 2.178 \times 10^{-12}s$, and $\tau_v = 1.029 \times 10^{-12}s$. We show the variations of TED in different Figures.

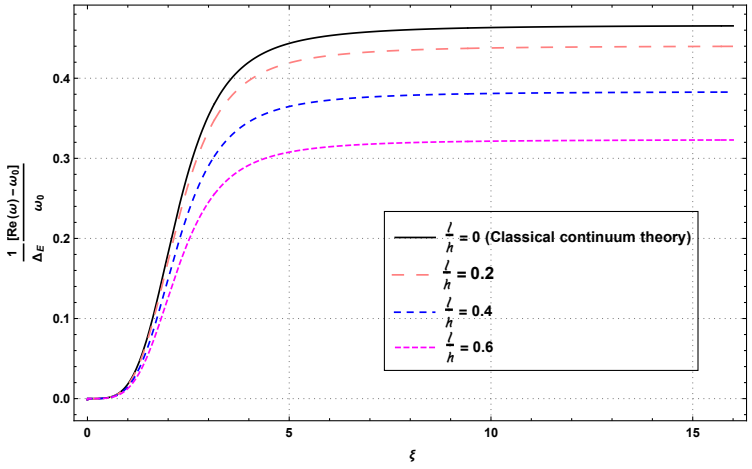

Figure 6.4.1: Behavior of normalized frequency shift ($[Re(\omega) - \omega_0]/\omega_0\Delta_E$) as a function of dimensionless variable ξ.

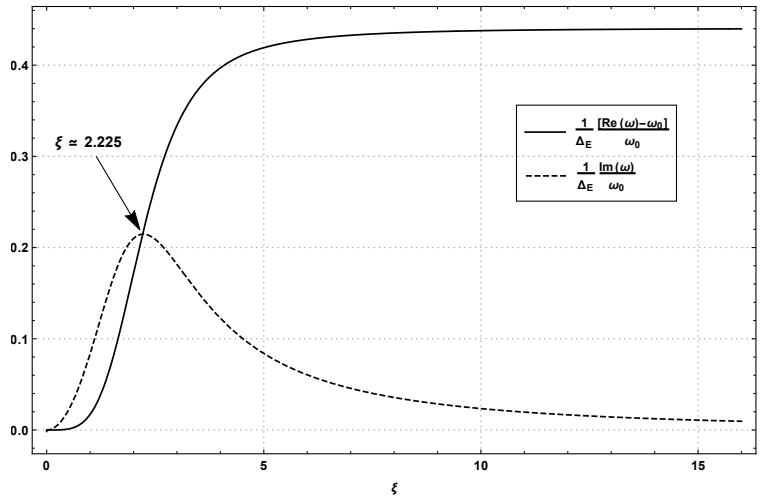

Figure 6.4.2: Behavior of normalized frequency shift $([Re(\omega) - \omega_0]/\omega_0\Delta_E)$ and normalized attenuation $(Im(\omega)/\omega_0\Delta_E)$ as a function of dimensionless variable ξ.

The plot of the normalized frequency shift is shown in Fig. 6.4.1 as a function of dimensionless variable ξ for the fixed aspect ratios $L/h = 40$ and $b/h = 25$. Here, the thickness of microplate resonator is fixed as $6\,\mu m$. We show here the variation with effects of the length-scale parameter, l by taking $l/h = 0$,0.2, 0.4 and 0.6. It is observed that there is a significant effect of the length-scale parameter l and the size-dependent normalized frequency shifts $([Re(\omega) - \omega_0]/\omega_0\Delta_E)$ are lower under modified couple stress theory as compared to the classical continuum theory. Further, it has been observed that with the increase of material length-scale parameter l, the normalized frequency shift decreases significantly.

Figure 6.4.2 shows the variation of the normalized frequency shift $([Re(\omega) - \omega_0]/\omega_0\Delta_E)$ and the normalized attenuation $(Im(\omega)/\omega_0\Delta_E)$ with respect to dimensionless variable ξ for fixed aspect ratios taken as $L/h = 40$, $b/h = 25$ with the thickness $h = 6\,\mu m$. This Figure depicts that the normalized attenuation of microplate resonators first increases and after showing a maximum peak value of TED, it decreases with the increase of ξ to attain a constant value. It is found out that there exists a critical frequency at which normalized attenuation attains its maximum peak value. Further, the normalized

frequency shift intersects with the normalized attenuation near this critical frequency, $\xi \backsimeq 2.225$ which is approximately the same as reported by Lifshitz and Roukes (2000) for generalized thermoelasticity with one relaxation time.

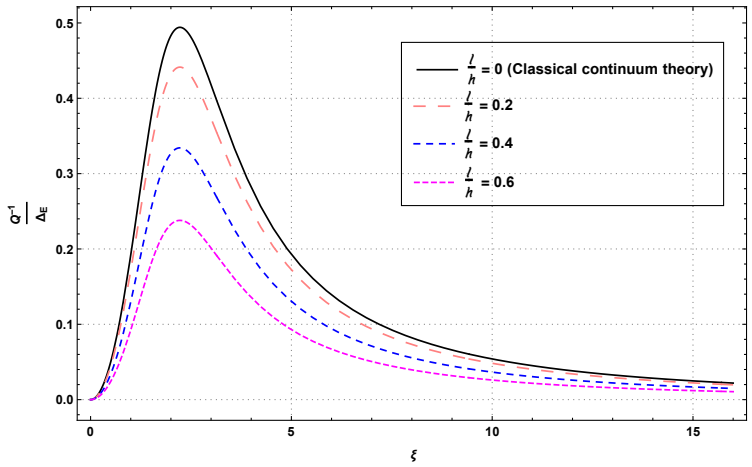

Figure 6.4.3: Variation of TED in microplate resonator with different values of $\frac{l}{h}$ as a function of the dimensionless variable ξ for first mode ($m = 1$, $n = 1$).

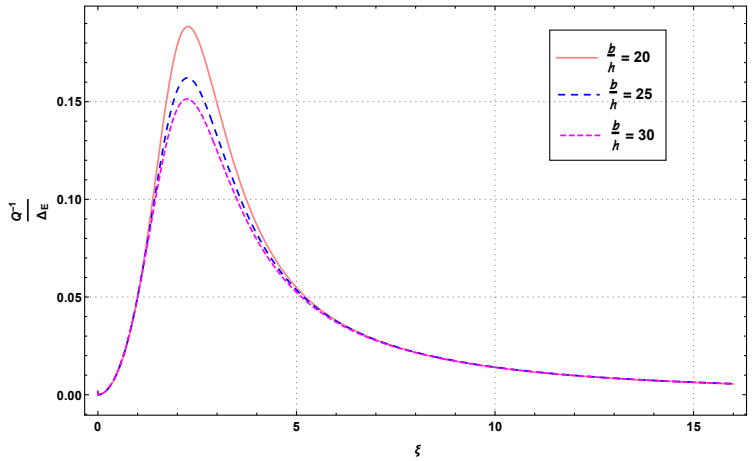

Figure 6.4.4: Variation of TED in microplate resonator with different values of $\frac{b}{h}$ as a function of the dimensionless variable ξ for first mode ($m = 1$, $n = 1$).

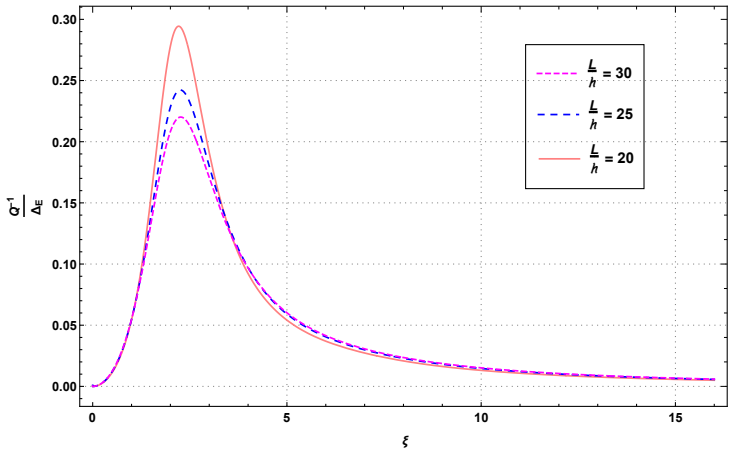

Figure 6.4.5: Variation of TED in microplate resonator with different values of $\frac{L}{h}$ as a function of the dimensionless variable ξ for first mode ($m = 1$, $n = 1$).

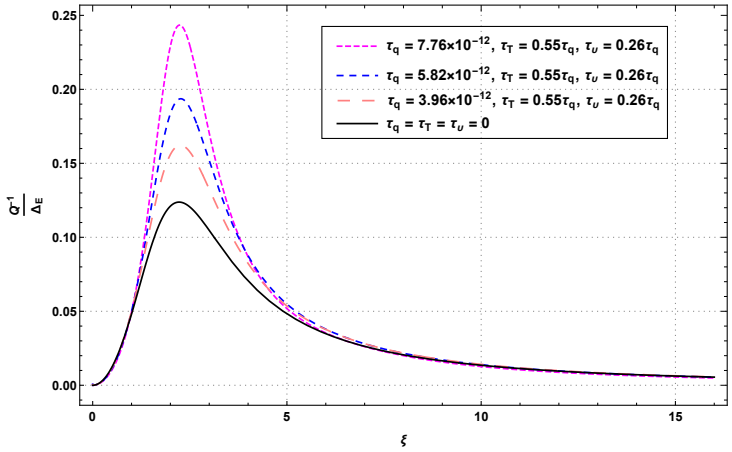

Figure 6.4.6: Variation of TED as a function of dimensionless variable ξ for different values of phase-lag parameters in case of simply supported (SSSS) boundary condition for first mode ($m = 1$, $n = 1$).

Figure 6.4.3 displays the variation of TED of microplate for different aspect ratios l/h ($l/h = 0$, 0.2, 0.4, 0.6) as a function of dimensionless variable ξ for the first mode ($m = 1$, $n = 1$). The Figure is plotted for fixed value of microplate thickness $h = 6\,\mu m$ and the fixed aspect ratios $L/h = 40$ and $b/h = 25$. It has been observed that the TED

first increases and attaining a peak value, it starts decreasing and finally tends to a constant value. It is indicated that MCST gives lower values of TED in comparison to the classical continuum theory $(l = 0)$. It is also evident that when l/h increases, the peak value of TED decreases significantly. A similar fact has been reported by Zhong et al. (2015) in case of classical coupled theory. It is also noted that the peak value of TED occurs near the critical value of normalized frequency $\xi = 2.225$. Interestingly, the critical value is not changed with change in the aspect ratio l/h.

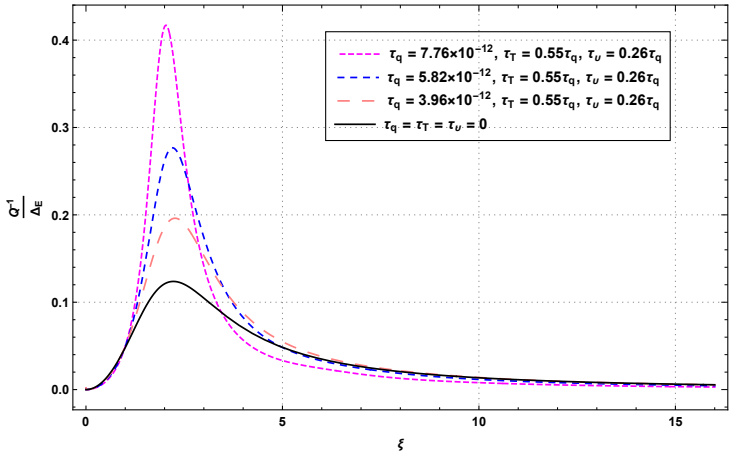

Figure 6.4.7: Variation of TED as a function of dimensionless variable ξ for different values of phase-lag parameters in case of clamped-clamped (CCCC) boundary condition for first mode $(m = 1, n = 1)$.

Figure 6.4.4 shows the variation of TED versus ξ for various aspect ratios b/h ($b/h = 20, 25, 30$) and for fixed value of aspect ratio of length-scale parameter and microplate thickness $l/h = 1$. Here, the length of microplate resonators is fixed as $L = 40\,\mu m$. From the variation of TED in this Figure, it can be concluded that TED decreases with the increase of aspect ratio b/h and hence the peak value decreases significantly. Furthermore, the value of the quality factor increases with the increase of the width of microplate resonator. The existence of critical value in ξ is observed in this case too. However, the position of critical value is unaffected with variation of

aspect ratio b/h.

In Figure 6.4.5, the dependence of the TED on the length of the microplate are depicted for different values of L/h (L/h = 20, 25, 30). Here, the thickness is fixed as $h = 0.01\,\mu m$ and the aspect ratio $b/h = 20\,\mu m$ is fixed. Also, the influences of the length of the microplate on the quality factor are shown for fixed aspect ratio $l/h = 1$. From Figure, it is clear that the amplitude of TED decreases with the increase in aspect ratio L/h. Hence, the dissipation of energy occurs more slowly with an increase in the length of microplate.

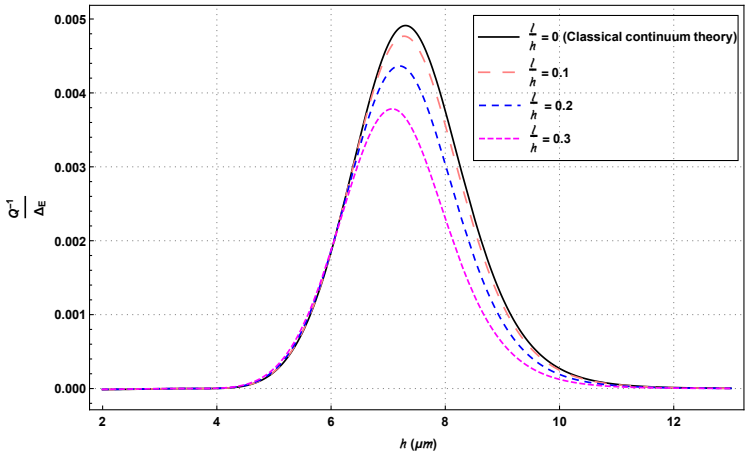

Figure 6.4.8: Variation of TED in microplate resonator with different values of $\frac{l}{h}$ as a function of the thickness h for first mode.

Figures 6.4.6 and 6.4.7 depict the effects of phase-lag parameters on TED as a function of dimensionless variable ξ for fixed $h = 0.01\mu m$, $l/h = 1$, $L/h = 40$, and $b/h = 25$. Fig. 6.4.6 shows the case of simply supported (SSSS) boundary condition, while Fig. 6.4.7 shows the influence of phase-lag parameters in case of clamped-clamped (CCCC) boundary condition. Figs. 6.4.6 and 6.4.8 clearly indicate a prominent influence of phase-lag parameters on TED in both the cases. It has been observed that when the values of phase-lag parameters increase, the TED increases and hence, the peak value increases. This implies that the quality factor decreases due to an increase in the val-

ues of phase-lags. It can be concluded that energy dissipation occurs more slowly with small values of phase-lag parameters. Furthermore, it is observed that there is more influences of phase-lags on TED in the case of clamped-clamped boundary condition as compared to the case of simply supported (SSSS) boundary condition.

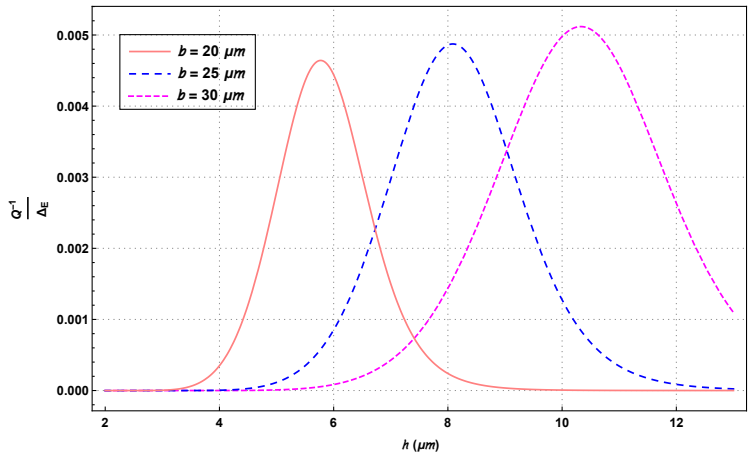

Figure 6.4.9: Variation of TED in microplate resonator with different values of b as a function of the thickness h for first mode.

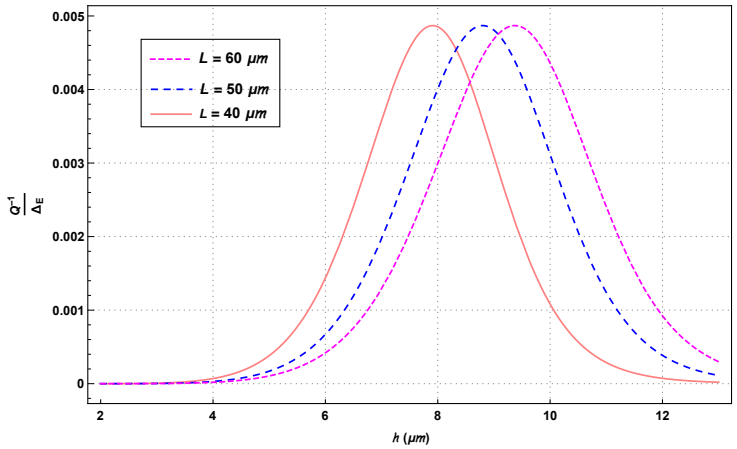

Figure 6.4.10: Variation of TED in microplate resonator with different values of L as a function of the thickness h for first mode.

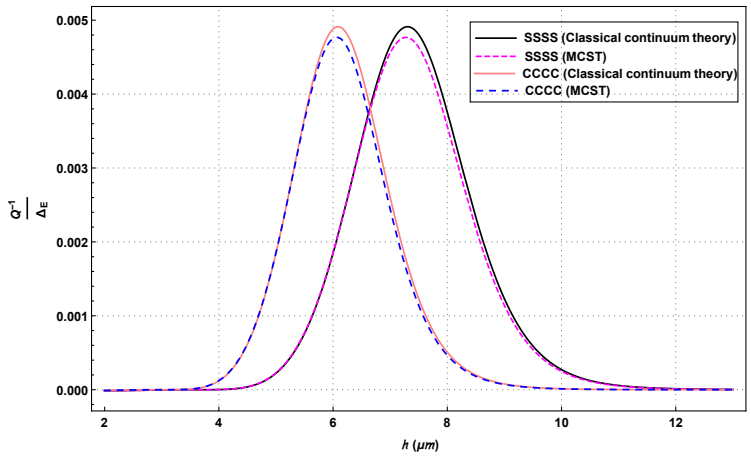

Figure 6.4.11: Variation of TED in microplate resonator with $l = 1\,\mu m$ as a function of the thickness h for simply supported and clamped edges of the microplate for first mode.

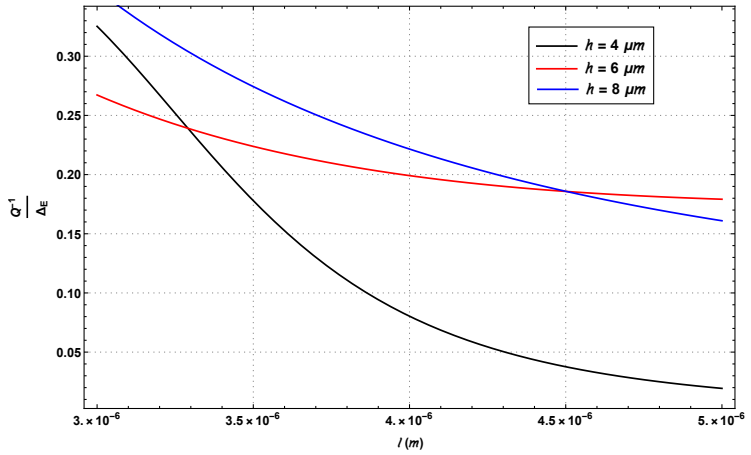

Figure 6.4.12: Variation of TED in microplate resonator with different values of the microplate thickness h as a function of the length scale parameter l for first mode.

The variation of TED in microplate resonators versus the thickness for the first mode is displayed in Fig. 6.4.8. Here, the length of the microplate and the normalized frequency are assumed to be fixed as $L = 40\,\mu m$ and $\xi = 2.225$, respectively. The Figure is plotted for various values of aspect ratio l/h ($l/h = 0$, 0.1, 0.2, 0.3). It has

been observed that MCST gives higher values of the quality factor in comparison to the values of the quality factor calculated by the classical continuum theory. This is evident from this figure which shows that the values of TED calculated by MCST are lower than those calculated by classical continuum theory. Moreover, the peak value of TED decreases by increasing the aspect ratio l/h. We note that when length-scale parameter increases, the dissipation of energy occurs more slowly. From Figure 6.4.8, it can be further found that the difference between the results of the MCST and classical continuum theory is significant when the thickness of the plate is close to the material length-scale parameter.

The variation of TED versus microplate thickness is plotted in Fig. 6.4.9 for different width b ($b = 20\,\mu m$, $25\,\mu m$, $30\,\mu m$) of the microplate. Here, the length-scale parameter is assumed to be $1\,\mu m$ and the length of the microplate is fixed as $L = 40\,\mu m$. It is evident that when the width b increases, the peak value of TED increases considerably. Hence, the prediction of the quality factor is lower for larger width of the microplate resonators.

Figure 6.4.10 indicates the variation of TED with respect to plate thickness h for variation in the plate length L ($L = 40\,\mu m$, $50\,\mu m$, $60\,\mu m$). The graph is plotted under the assumption of $l = 1\,\mu m$, $b = 30\,\mu m$, and the normalized frequency $\xi = 2.225$. It can be seen that the peak value of TED remains approximately the constant and unaffected due to change in the length of microplate. However, the critical thickness showing the peak value is shifted towards right when we increase the length of the plate. A similar fact has been reported by Borjalilou and Asghari (2018) in the context of dual phase-lag theory.

Figure 6.4.11 reveals the nature of variation of TED as a function of plate thickness for different values of plate width $b = 25\,\mu m$ and length $L = 40\,\mu m$. Here, we present the effect of applying the simply supported (SSSS) and clamped-clamped (CCCC) boundary conditions on TED. In this case, we have fixed the normalized frequency as

$\xi = 2.225$. The length-scale parameter is also assumed to be $1\,\mu m$. It is clear that the maximum peak values of TED are approximately the same for both the boundary conditions. Furthermore, the peak values of TED calculated by MCST is less than the peak values obtained by classical continuum theory in case of both the boundary conditions. However, the critical thickness is larger for the case of SSSS boundary condition as compared to the case of CCCC boundary condition.

Figure 6.4.12 indicates the dependency of the quality factor on the length-scale parameter. The variation of TED is depicted for different values of microplate thickness $6\,\mu m$, $8\,\mu m$, and $10\,\mu m$. The Figure is plotted by considering $L = 40\,\mu m$ and $b = 25\,\mu m$. Fig. 6.4.12 verifies the fact that there is a significant effect of microplate thickness on TED . However, it is not a monotonic function of the microplate thickness. A similar fact has been reported by Zhong et al. (2014) in case of classical coupled theory and by Borjalilou and Asghari (2018) in case of dual-phase-lag theory.

6.5 Conclusion

In the present work, an explicit general formula for the quality factor has been derived on the basis of MCST and the TPL heat conduction model to investigate the nature of energy dissipation in a rectangular microplate resonator. An analytical expression for TED has been derived by complex-frequency approach. To study the small scale-effects on TED, the numerical results of the present model have been compared with the corresponding results of classical continuum theory. The effects of different parameters of microplate resonators on the TED such as thickness, normalized frequency, aspect ratio, length-scale parameter, boundary conditions have been discussed in detail. Furthermore, the effects of phase-lag parameters on TED have also been presented. The main observations of the present work are highlighted below:

- The prediction of the values of the quality factor utilizing MCST is higher than

the classical continuum theory.

- With the increase of the material length-scale parameter, the quality factor increases significantly from the classical continuum theory.
- It is demonstrated that the results of the present model diverge from the classical continuum theory when the thickness of microplate resonators is close to material length-scale parameter.
- By fixing the width of microplate resonators as constant, there is a significant difference in the quality factor, but the peak values are approximately the same.
- There is a significant effect of boundary condition on the TED of microplate resonators. However, the peak values of TED are approximately the same for simply supported and clamped-clamped boundary conditions when the normalized frequency is fixed.
- With the increase in the values of phase-lag parameters, the quality factor decreases significantly as a function of normalized frequency.
- Modified couple stress theory with small values of phase-lag parameters can increase the quality factor of microplate resonators with a smaller thickness.